Numerical Simulations and Observations of the Internal Tide in a Submarine Canyon

Leslie K. Rosenfeld and Jeffrey D. Paduan
Naval Postgraduate School, Monterey, California

Emil T. Petruncio
Naval Meteorology and Oceanography Command, Stennis Space Center, Mississippi

J. Eduardo Goncalves
University of São Paulo, Brazil

Abstract. Observations and model simulations of internal waves in and around the Monterey Canyon are described here with particular focus on the internal tide generated through interaction of the basin-scale barotropic tide and local topography. Observations reveal strong internal tides along the axis of the Canyon near the Canyon head. Currents are intensified near the bottom and observed to have both onshore-propagating and standing configurations at different times and stratification conditions. Bottom-mounted ADCP observations from within the Canyon axis in depths around 300 m confirm bottom intensified fluctuations throughout the internal wave band. Furthermore, strongly nonlinear fronts or bores are associated with the tidal-band fluctuations. Numerical simulations forced by semidiurnal sea level fluctuations offshore using both idealized and realistic representations of the local topography are used to investigate internal tide generation and propagation in the coastal zone. Canyons with near-critical bottom slopes play a role in bottom intensification, while the actual complex topography leads to significant horizontal variations in the internal wave characteristics on scales of less than 10 km.

1. Introduction

In the proceedings from a previous 'Aha Huliko'a Workshop, *Hickey* (1995) reviewed what was known about circulation in and around submarine canyons. In this paper we focus on a particular canyon, the Monterey Canyon (MC) off central California (Figure 1). We present the current state of knowledge pertaining to the internal wave field in MC, with emphasis on the internal tide both from an observational and modeling perspective. The head of MC lies within 100 m of Moss Landing harbor (Figure 2). Within the confines of Monterey Bay the axis of the Canyon lies, with some meandering, in the cross-shore direction (080°-260°T), bisecting the Bay. Between the mouth of the Bay and the Canyon head, a distance of approximately 20 km, the floor of the Canyon rises from 1000 m to 100 m with a slope that varies between 1.7-2.6°. Over the same distance, the Canyon width (defined as the distance between the 150 m isobaths on the Canyon rims) decreases from approximately 11 km to nearly 2 km.

Monterey Bay sea level fluctuations are characterized by a mixed, predominantly semidiurnal tide. The sea level throughout the Bay essentially co-oscillates. The largest constituent, M_2, has an amplitude of 49 cm, and the second largest constituent, K_1, has an amplitude of 24 cm (*Petruncio*, 1993). While previous CTD observations indicated the presence of large internal tides in Monterey Canyon (*Broenkow and McKain*, 1972), it was surface current data derived from HF radar (CODAR) that inspired our interest in this topic. Tidal analysis of several 30-d periods of surface current records revealed semidiurnal currents an order of magnitude larger than expected (10' s of cm s^{-1} as opposed to a few cm s^{-1}) based on sea level amplitudes, and perhaps more interestingly, the semidiurnal surface currents were out of phase with what one would expect from looking at sea level;

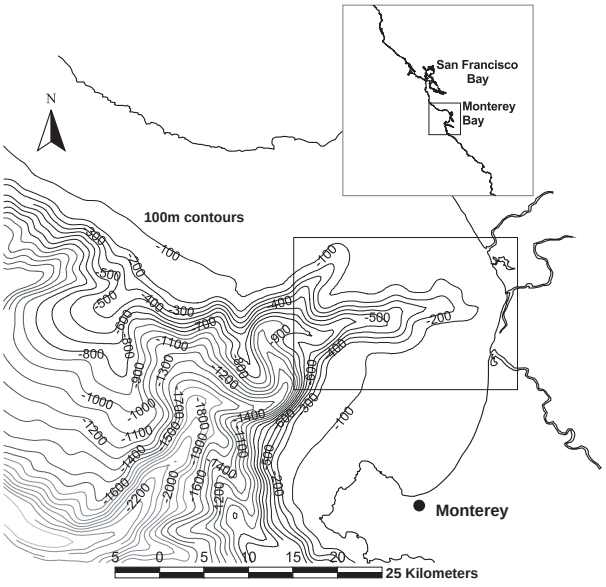

Figure 1. The Monterey Bay, California study site. Canyon measurements described here are from the area within the rectangular box.

i.e. the surface currents flowed out of the bay during sea level rise (*Paduan and Cook*, 1997; *Petruncio et al*., 1998).

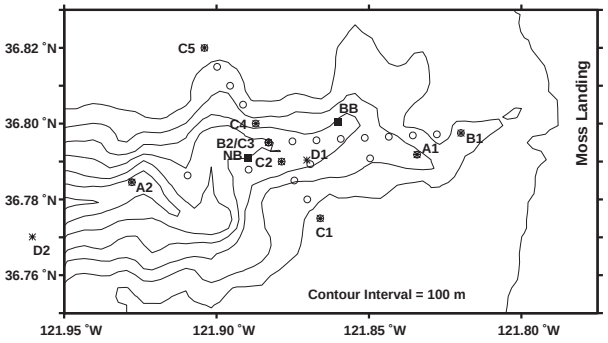

Figure 2. Map showing the locations of the CTD (*) and VM-ADCP (O) measurements made during ITEX1 (A) , ITEX2 (B and C) and MCIW (D). Moored ADCP and temperature measurements were made at BB and NB during MCIW. Depth contours relative to the measurement locations are not highly accurate due to the low resolution of the bathymetry in this figure.

It has long been known, both from theory and observations, that submarine canyons may serve as "traps" for internal wave energy (*Gordon and Marshall*, 1976; *Wunsch and Webb*, 1979; *Hotchkiss and Wunsch*, 1982 among others). These environments, being notoriously inhospitable places to make measurements, typically have observations restricted to fairly short durations, on the order of a few days. Where longer time series do exist (*Hotchkiss and Wunsch*, 1982; *Hunkins*, 1988; *Hickey*, 1989; *Noble and Butman* 1989; *Hickey*, 1997 among others), the temporal resolution is generally not fine enough to resolve the highly nonlinear aspects of the flow, nor the high frequency end of the spectrum.

2. Internal Tide Experiments – 1994

2.1. Methods

Our initial investigations consisted of 25-50 h time-series of velocity and density constructed from shipboard ADCP and CTD measurements described in *Petruncio et al*. (1998). During Internal Wave Experiment 1 (ITEX1) in April 1994, CTD stations spaced 8.3 km apart along the canyon axis were occupied every 1.5-2 h for 25 hours (Figure 2). During ITEX2 in October 1994, the CTD stations were located closer together (5.6 km apart) and closer to shore. In ITEX2, the along-canyon measurements were followed by another 25 h of cross-canyon CTD and ADCP surveys. The CTD stations were positioned so that the deeper axial station was common to both the along- and cross-canyon measurements, allowing construction of a time series 50 h in length at that site. The remaining cross-canyon stations were located above the Canyon walls and in the shallow water (60-90 m) on the flanks of the Canyon. The velocity data were spatially averaged by assigning the measurements to evenly spaced along-track geographic bins of 1.5 km for ITEX1 and 0.7 km for ITEX2. The cross-track width of these bins was no more than 0.5 km. The one-minute ensembles in each geographic bin were temporally averaged so that the sampling interval at each de facto ADCP station was the same as that of the CTD stations, 1.5-2 h. A 150 kHz RD Instruments vessel-mounted ADCP with an array of four transducers oriented 30° from the vertical in a Janus configuration was used. Although the ADCP is capable of measuring to depths greater than 400 m, data within the lower 20-30% of the water column can not be used due to side lobe interference from reflections off the Canyon floor and walls.

2.2. Results

Both experiments revealed that semidiurnal kinetic and potential energy was elevated in a 150-200 m-thick band centered 150 m above the bottom, with current amplitudes of 15-20 cm s^{-1} (Figure 3). This conclusion is limited however by the vertical extent of the velocity data, which did not include the lower part of the water column. The angle the characteristic ray paths, or beams, make with the horizontal was computed from the velocity and density time-series five different ways, and all gave an answer close to 2.3° (*Petruncio et al*., 1998). Energy maxima lay nearly parallel to the large-scale canyon floor slope, as do the ray paths computed from linear theory using the measured averaged N^2 profiles. The horizontal wavelengths were estimated to be 30 km, and the group velocities 50-55 cm s^{-1}. A significant difference between the two experiments is that, in the first, energy appeared to propagate shoreward parallel to the canyon floor and was best described as a beam. In the second experiment, while the energy maxima were still parallel to the canyon floor, the amplitude and phase structures indicated a standing wave (Figure 4), more easily described in terms of a small number of low modes. At the time we speculated that this difference in vertical structure might be due to seasonal differences in stratification. There is also some evidence to suggest that there is phase-locking between the surface and internal tide. Higher energy levels were observed during the spring tide conditions of ITEX1, versus the neap tide conditions of ITEX2. Cross-canyon measurements made during ITEX2 revealed the internal tide can act to transport cold dense water up onto the shelves to the sides of the Canyon as suggested by *Shea and Broenkow* (1982).

It is difficult to determine whether the internal tide energy in MC is locally generated, or propagates in from another region, and then is concentrated there due to the steep canyon walls and near-critical bottom slope. The fact that the observed energy maxima were elevated above the canyon floor provides some indication of non-local generation. Figure 5 shows the ray paths emanating from an area to the west of the ITEX sites where the bathymetry is near critical for the M_2 frequency over a large spatial area. We speculated that "Smooth Ridge" could have been the source for the internal tide energy we observed. The figure also illustrates the significant sensitivity of the M_2 ray paths to the different stratifications observed in ITEX1 and ITEX2.

3. Model Simulations with Idealized Bathymetry

In order to investigate further internal tide generation and propagation in a submarine canyon, we used a primitive

equation numerical model, the Princeton Ocean Model (POM). At least two previous investigators have used POM to investigate internal tides in the coastal ocean. *Holloway* (1996) used a two-dimensional implementation to study internal tide generation and propagation on the Australian North West Shelf. *Cummins and Oey* (1997) used a fully three-dimensional implementation to look at barotropic and baroclinic tides off northern British Columbia.

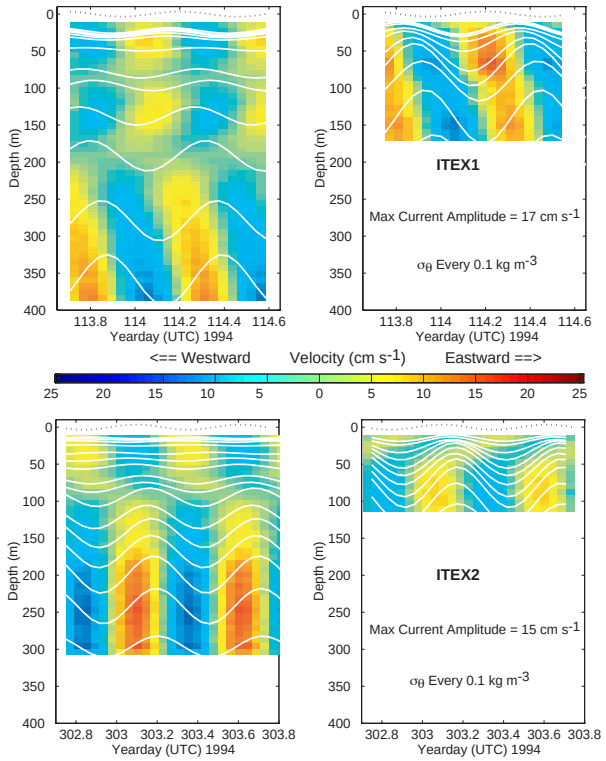

Figure 3. Time series of semidiurnal component, as determined from least-squares fit to the M_2 frequency, of east-west velocity component and isopycnal displacements for deep station A2 (upper left) and shallow station A1 (upper right) during ITEX1 and deep station B2 (lower left) and shallow station B1 (lower right) during ITEX2. Demeaned M_2 sea level oscillations exaggerated by a factor of 10 (dashed lines) are also shown.

3.1. Model Setup

We used a 70 km x 70 km domain with a simplified geometry including a 2500 m deep basin, a continental slope with a maximum gradient of 7.15°, and a 20 km wide shelf, 100 m in depth (Figure 6). The eastern boundary of the domain, which represents the coast, was the only closed boundary. The shelf and slope were incised by a single canyon perpendicular to the coast. In the case discussed here, the canyon floor was inclined 1.55° from the horizontal and was 3 km wide. The width across the top of the canyon varied along its length from 11 km at the mouth to 3 km at the head. Horizontal resolution of 1 km x 1 km with 30 σ-levels was used throughout the domain. The σ-levels were logarithmically distributed near the surface and bottom, with vertical resolution in the boundary layers ranging from 12.5 m over the basin to 0.5 m over the shelf. In the middle of the water column (σ-levels 5-26), vertical resolution ranged from 107.5 m over the basin to 4.3 m over the shelf. An external time step of 2 s and an internal time step of 120 s were used. The initial temperature and salinity fields were constant in the horizontal but had vertical dependence typical of summertime stratification conditions in the vicinity of Monterey Bay.

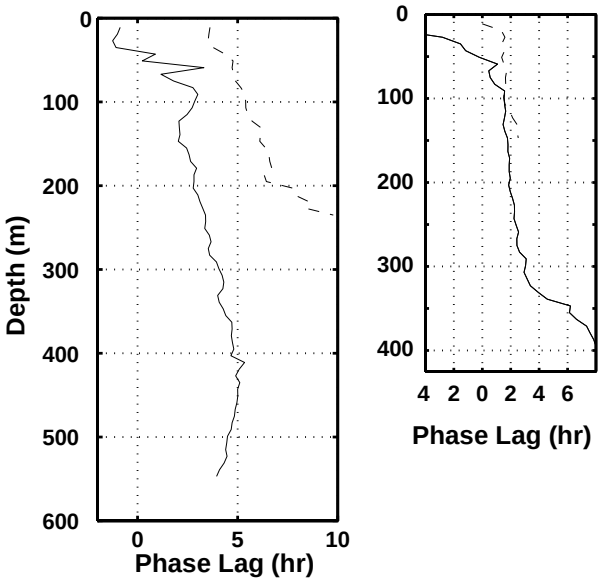

Figure 4. Phase of M_2 component of isopycnal displacement for the deep (solid; A2, B2) and shallow (dashed; A1, B1) CTD time-series stations made over the Monterey Canyon axis during ITEX1 (left) and ITEX2 (right).

A complete description of these model runs can be found in *Petruncio* (1996). The model was forced with only one tidal constituent, the M_2, applied as a 0.5 m-amplitude cosine wave to sea level at the western boundary. The model was run for four days with output from the last three semidiurnal cycles used in the analyses summarized below. A mixture of boundary conditions were used. Radiation conditions were applied to the external mode velocities and to the internal mode velocities on the northern and southern boundaries. On the offshore (western) boundary, internal mode velocities and density gradients were decayed exponentially to zero over a 10 km-wide sponge region parallel to the boundary.

3.2. Model Results

Figure 7 shows that in the model results the energy maximum lies at, or near, the canyon floor and is bounded on the upper side by the characteristic emanating from the foot of the canyon. The characteristic lies nearly parallel to the canyon floor, thus trapping energy generated at the foot along the bottom. In addition, internal tide energy is generated along the portion of the canyon floor critical with respect to the M_2 frequency. (The canyon floor slope is constant but the density stratification varies with depth, thus making only that part of the canyon floor near 300 m depth critical.) A comparison between ITEX1 observations and the model results is shown in Figure 8. Although the model underpredicts the current amplitude by about 50% (due to a

combination of simplifications in the model bathymetry, forcing, and density variability relative to the real ocean), the structure looks very much the same, indicating upcanyon energy propagation parallel to the canyon floor. The phase lag between the model currents and sea level is within 1/4 cycle of that observed in ITEX1; near the head of the canyon, maximum shoreward flow occurs in the lower half of the water column, close to the time of high tide. It is not surprising that the phase difference between sea level and maximum upcanyon current is different in the model than the observations since this is so strongly a function of where the measurement site is relative to the generation site.

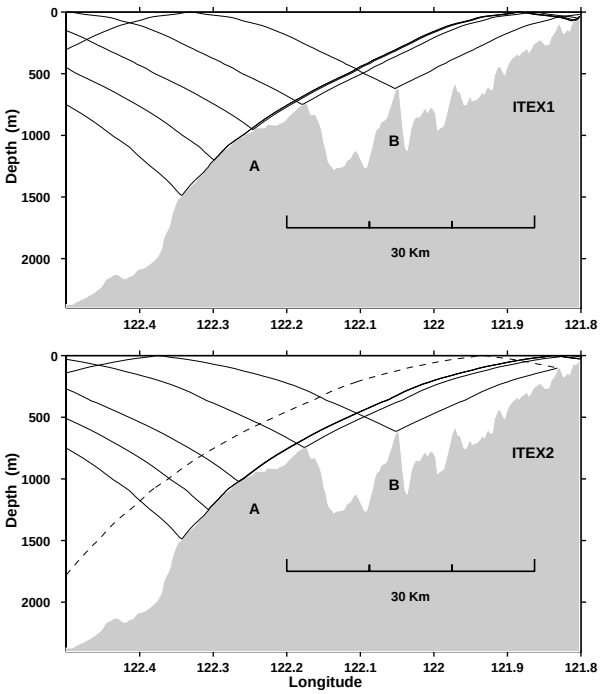

Figure 5. M_2 characteristics calculated from the linear internal wave dispersion relation showing possible paths of energy propagation from Smooth Ridge (A) and Steep Ridge (B) into MC. The dashed line represents a reflected ray.

As suggested by the observations, isopycnal displacements associated with the internal tides (5-10 m in the model) move water from beneath the canyon rim up onto the shelf. As the isopycnals sink back down below the rim, lenses of dense water pinch off and remain on the shelf in the manner suggested by *Shea and Broenkow* (1982). This "tidal pumping" along the rim of the model canyon near its head is clearly a source of alongshore-propagating internal tides (not shown), which transition from beam-like near the generation site at the canyon rims to first-mode-like near the model boundaries. The density field in the bottom boundary layer at 200-300 m depth reveals that upcanyon-propagating bore-like surges occur along the canyon floor during rising tide, resulting in isopycnal displacements of 5-10 m. This boundary layer activity is consistent with the 2-D numerical simulations of *Slinn and Riley* (1996), who observed that critical angle internal wave reflection on floors with shallow slopes (3.4°-9°) resulted in the upslope propagation of thermal fronts in the bottom boundary layer.

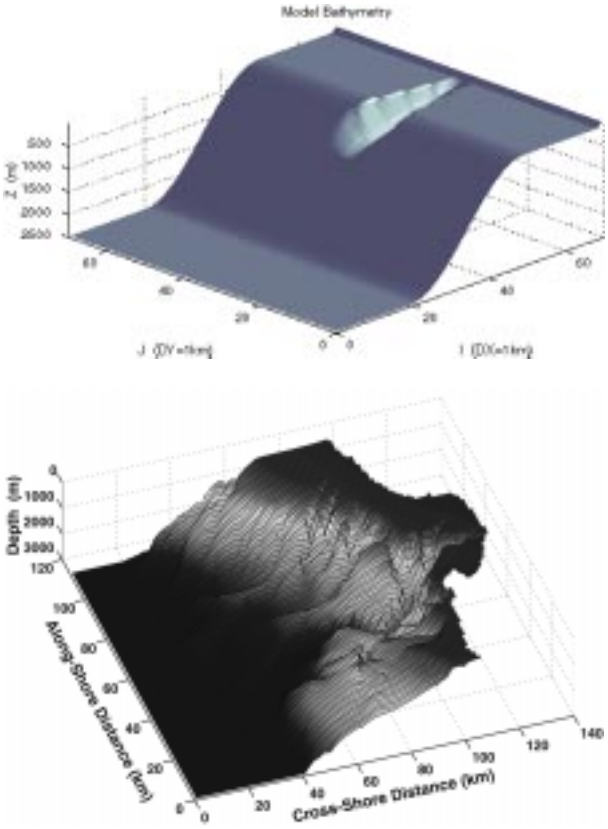

Figure 6. Model geometry and bathymetry for the idealized case (top) featuring a straight coast and shelf with a canyon incising the slope and shelf at a right angle, and a realistic case (bottom) featuring the Monterey Canyon and Bay.

4. Internal Wave Experiment – 1997

At the conclusion of the previously described work, it was clear that the near-bottom region, undersampled in the previous studies, was likely to contain high levels of energy and shear associated with internal wave generation, trapping, and reflection. In August-September 1997, as part of the Monterey Canyon Internal Wave Experiment (MCIW), Rosenfeld deployed two moorings at 390 and 337 m depth with upward-looking ADCPs and near-bottom thermistors, in the same vicinity of MC where ITEX1 and ITEX2 took place (Figure 2). Twelve-hour CTD time series with 30-min resolution were made about halfway between the two moorings at station D1 on 9 August and 21 August. The 34-d velocity and temperature records, with temporal resolution of 1-3 minutes, confirmed the bottom-intensification of the internal tide, but also revealed for the first time the highly nonlinear character of the signal. High-resolution bathymetry data (vertical resolution of 0.1% of water depth and horizontal resolution of 2% of water depth) obtained by the Monterey Bay Aquarium Research Institute during the summer of 1998, shows that the shallower mooring, BB, was located near a bend in the canyon, thus explaining the highly asymmetric flow measured there (Figure 9). "Along-canyon" flow was calculated for the deepest 4-m bin, centered 12 m above the bottom, by projecting the velocity vectors in the northeast and

southwest quadrants onto the major principal axis computed from all the points in the northeast quadrant (positive eastward), and projecting the velocity vectors in the northwest and southeast quadrants onto the major principal axis computed from all the points in the northwest quadrant (negative westward). This results in a scalar time series with upcanyon (eastward) flow being positive and downcanyon (westward) flow being negative.

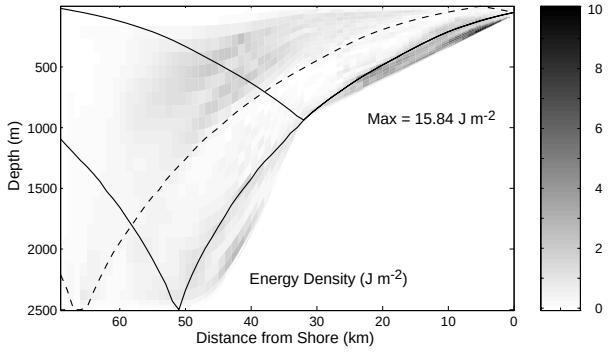

Figure 7. Along-canyon section of M_2 energy density with characteristics emanating from the shelf break (solid lines) and reflecting from the coastal boundary (dashed lines).

"Internal bores," visible as sharp drops in temperature with coincident accelerations in the along-canyon velocity (Figure 10) occur at 11-13 h intervals throughout much of the record at mooring BB. They are particularly prominent and regular during the last 8 days of the time-series, which interestingly does not coincide with the times of maximum tidal range in sea level. There is also circumstantial evidence from a 12-h CTD time series taken between the two moorings that a decrease in light transmission follows the bore passage. At the deeper mooring, NB, the temperature drop takes place as two smaller steps.

These data clearly show that the kinetic energy in the internal wave band throughout the lower third of the water column (the entire range measured by these bottom-mounted upward-looking ADCPs) is elevated above the G-M spectra (Figure 11) calculated according to:

$$E_{GM} = \left[\frac{E_0 b^2}{\pi}\right] \frac{N_0}{N(z)} f \frac{(N^2 - \omega^2)(\omega^2 + f^2)}{\omega^3 \sqrt{\omega^2 - f^2}} \qquad (1)$$

using the canonical values (*Munk*, 1981) for b (1.3 km), N_0 (5.2 x 10^{-3} s^{-1}), E_0 (6.3 x 10^{-5}), the appropriate value of f for this latitude, and $N(z)$ calculated from the two 12-h averaged density profiles. Although G-M predicts slightly lower energy levels at 12 m above bottom relative to 112 m above bottom (based on the density profile), the opposite is observed. The energy decreases as you get further up in the water column, and the tidal signal becomes more linear, as evidenced by the reduction in the energy in the overtides. In general the spectral shape follows a ω^{-2} slope, except for the peaks associated with the tides and overtides.

We also found that the vertical structure, as seen in isopycnal displacements derived from two CTD time series made just 12 days apart (Figure 12), exhibited changes similar to those observed between ITEX1 and ITEX2, which differed in time by 6 months. This suggests that the stratification changes responsible for significant alterations to the internal tide may occur on synoptic time scales as well as on seasonal time scales. Indeed, significant changes in the stratification did take place between 9 and 21 August (most probably between 9 and 10 August based on CTD measurements made 10 km west of this site), although they primarily affected the top 250 m of the water column.

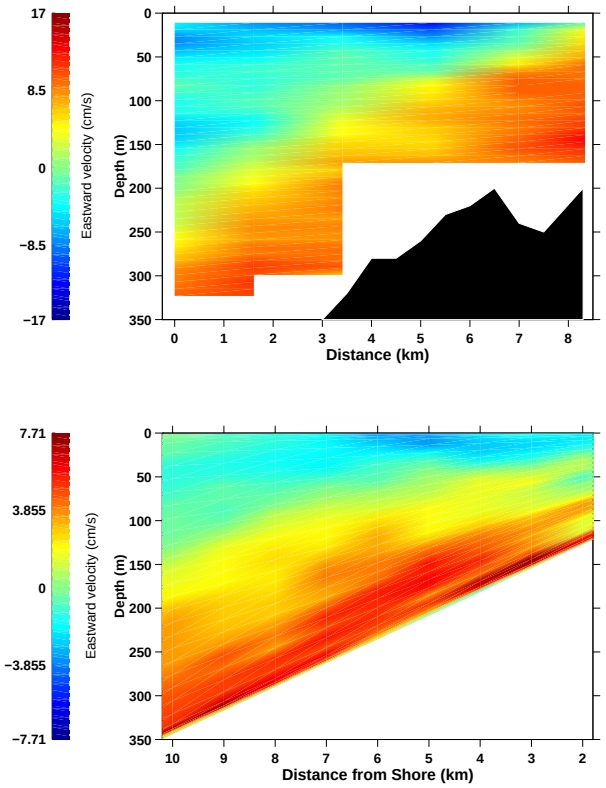

Figure 8. Along-canyon section of the model u at time of high tide (lower), and the u 2.5 h after M_2 high tide observed during ITEX1 (upper).

5. Model Simulations with Realistic Bathymetry

Coincident with our efforts to obtain more highly resolved observations of the internal wave field in MC, we have been pursuing more realistic model simulations of the same process. Still using POM with 30 vertical σ-levels and the forcing and stratification described above, we adopted a new grid using realistic bathymetry from a 250-m (horizontal) resolution data set (Figure 6). The domain size for these simulations was expanded to 130 km x 113 km and rotated about 20˚ to minimize land points, and to align the offshore boundary with the, approximate, along-shore direction. Difficulties with the sponge-type open boundary conditions limited the maximum depth in the model to 2500 m for these preliminary simulations.

The model was run for 10 days and the results of the last M_2 tidal cycle were used in the analyses presented here.

Critical to realistic generation of the internal tide for a particular high-resolution topographic domain is an accurate specification of the barotropic forcing, which interacts with the sloping bottom to generate internal waves.

We verified that the offshore sea level forcing we imposed acted to produce barotropic currents with magnitudes of 1-4 cm s^{-1} as expected from what is known about the basin-scale tidal currents (*Battisti and Clarke*, 1982). The depth-averaged current hodographs on day 10 of the model run are shown in Figure 13. In this case, the weak (<1 cm s^{-1}) cross-shore currents in the outer portion of the domain are accelerated to a maximum of 4 cm s^{-1} over the continental shelf in the northern part of Monterey Bay. The actual generation of internal waves in the model is proportional to the volume flux vector, $\vec{U}H$, where $\vec{U}$ is the depth-average velocity and H is the water depth (*Baines*, 1982). It is important to note that, although this simulation includes realistic cross-shore forcing, it does not include the along-shore component of the basin-scale tidal forcing. Given the complex topography of the Monterey Bay region, along-shore barotropic currents may be responsible for significant internal tide generation that should be included in future model simulations.

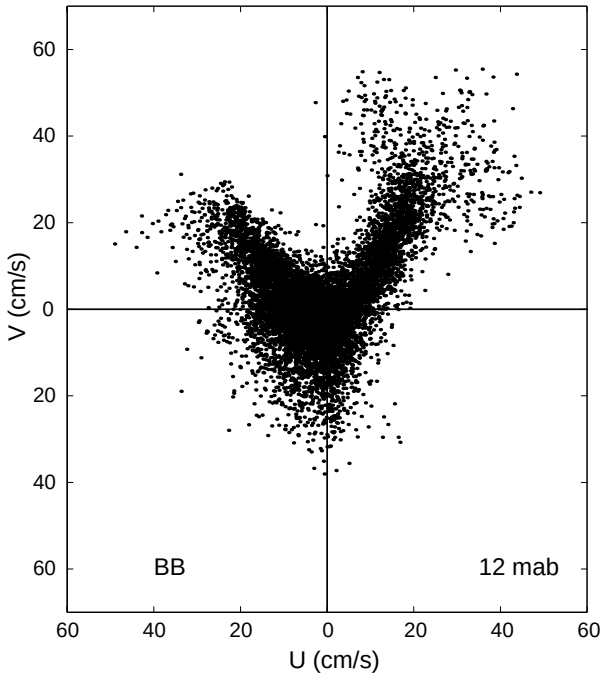

Figure 9. Scatter plot of velocity from the deepest 4-m bin, centered 12 m above the bottom, at mooring BB. Every third 1.5-min data point from the 34-d time-series is plotted.

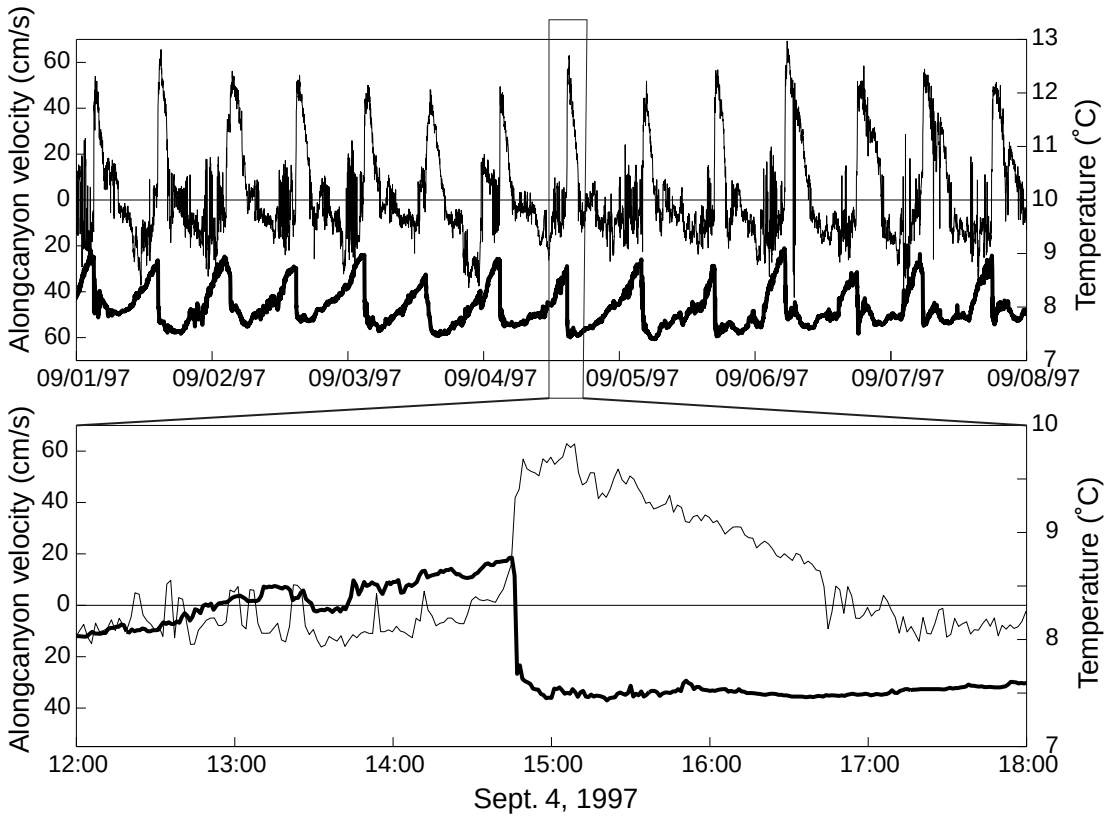

Figure 10. Temperature (bold line) measured once per minute 4 m above the bottom and along-canyon velocity (light line) averaged over 1.5-min intervals from the deepest 4-m bin, centered 12 m above the bottom, at mooring BB for one week (upper panel) and for a 6-h period within that week (lower panel).

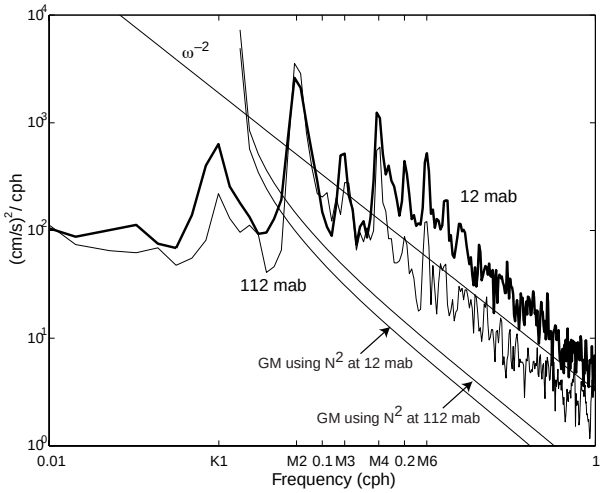

Figure 11. Kinetic energy spectra for the depth bins centered 12 and 112 m above the bottom at mooring BB, together with the G-M spectra calculated using values of *N* for these depths derived from the nearby CTD time series.

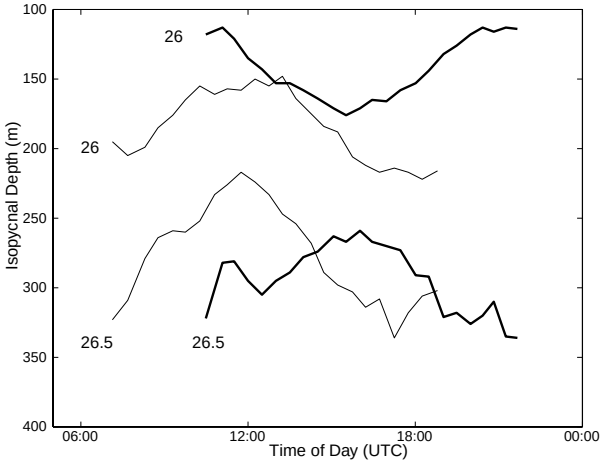

Figure 12. The σ_θ = 26.0 and 26.5 isopycnals versus time of day for 9 August (light) and 21 August (heavy) 1997 CTD time series.

This preliminary simulation using only offshore forcing does provide insights into the baroclinic response of this region to tidal forcing, particularly in the very interesting confines of the Canyon. Hodographs of the near-bottom currents during a semidiurnal tidal cycle on day 10 of the model simulation are shown in Figure 14 for the subset of the model domain within Monterey Bay. The current patterns are complicated, but they have a strong correlation with the bottom depth contours. The maximum currents exceed 12 cm s^{-1} and are found within the Canyon axis near the region of the ITEX measurements described above. These currents are four to ten times larger than the depth-averaged currents produced directly by the M_2 sea level forcing. The near-bottom current hodographs are much less elliptical than those of the depth-averaged currents, which suggests asymmetric flows for the upcanyon and downcanyon portions of the tidal cycle and/or significant nonlinear transfer to high-order tidal harmonics.

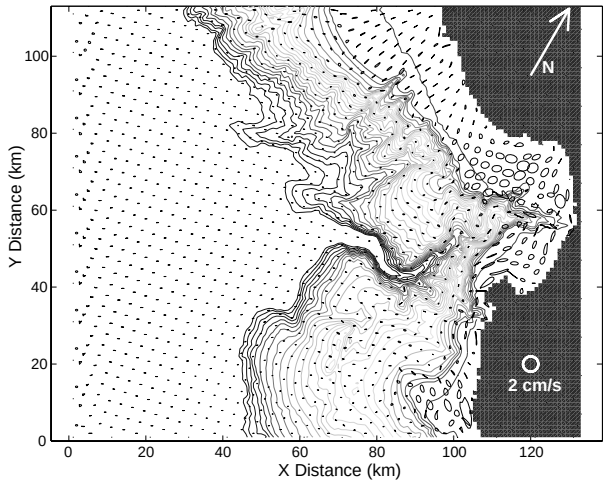

Figure 13. Depth-averaged current hodographs over a semidiurnal tidal cycle on day 10 of the POM simulation. Every 5th model grid point is shown. The contour interval is 100 m and the largest speeds are ~4 cm s^{-1} over the continental shelf.

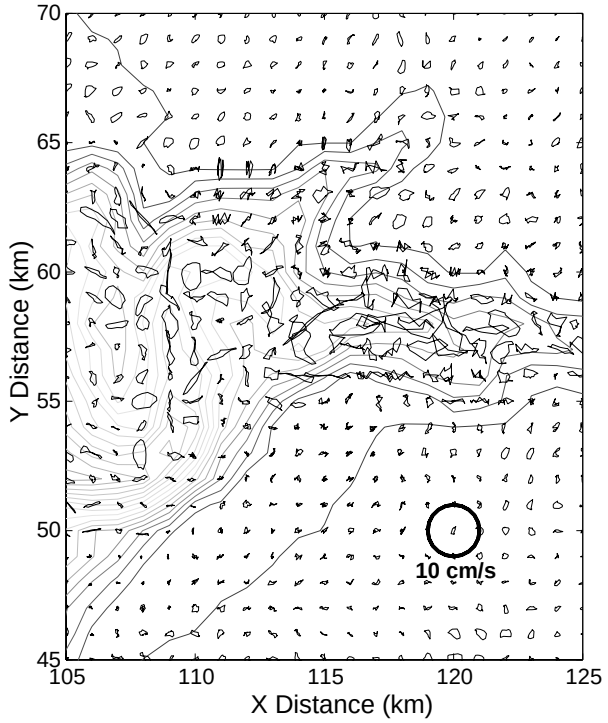

Figure 14. Bottom current hodographs over a semidiurnal tidal cycle on day 10 of the POM simulation. Every grid point is shown for the Monterey Bay portion of the model domain. The contour interval is 100 m and the largest speeds are ~12 cm s^{-1} in the axis of the Canyon.

6. Conclusions

Large isopycnal oscillations have been reported near the head of Monterey Canyon for more than 25 years (*Broenkow and McKain*, 1972). It has been shown that the internal tides

responsible for these also result in surface currents ten times as large, and of opposite phase, as the barotropic tidal currents (*Petruncio*, 1993). This is possible because of the bottom-intensified nature of the internal tidal signal (*Petruncio et al*., 1998) which is a consequence of the slope of the canyon floor being near-critical for the semidiurnal tidal constituents. Very near-bottom high temporal resolution measurements reveal the strongly nonlinear character of the signal. A hydrostatic primitive equation model (POM) is able to replicate many aspects of the observed internal tide; including the bottom-intensification and shoreward propagation of energy nearly parallel to the canyon floor. Further study using the realistic, complex topography should provide more information about the source regions for the internal tide, the dominant horizontal scales of variability, and the sensitivity of internal tide generation to the resolution of the actual bottom features over scales from 1 km to 10 km. However, since the model is hydrostatic, we would not expect it to accurately simulate the bore-like features now known to exist, or the details of the energy cascade within the higher frequency portion of the internal wave band. A combination of hydrostatic modeling at the generation scales with non-hydrostatic modeling of the energy cascade is expected to provide the most insights into the distribution of internal wave energy for a particular coastal regime.

Acknowledgments. We would like to thank Mike Cook, Scott Key, and Fred Bahr for assistance with data processing and display. We also gratefully acknowledge support from a NSF grant to Rosenfeld (OCE-9619466) and an ONR grant to Paduan and Rosenfeld (N00014-97WR-30009).

References

Baines, P.G., On internal tide generation models, *Deep-Sea Res., 29*, 307-338, 1982.

Battisti, D.S., and A.J. Clarke, A simple method for estimating barotropic tidal currents on continental margins with specific application to the M2 tide off the Atlantic and Pacific Coasts of the United States, *J. Phys. Oceanogr., 12*, 8-16, 1982.

Broenkow, W. W., and S. J. McKain, Tidal oscillations at the head of Monterey Submarine Canyon and their relation to oceanographic sampling and the circulation of water in Monterey Bay, Moss Landing Marine Laboratories Tech. Pub. 72-05, 42 pp., 1972.

Cummins, P. F., and L.-Y. Oey, Simulation of barotropic and baroclinic tides off northern British Columbia, *J. Phys. Oceanogr.*, *27***,** 762-781, 1997.

Gordon, R. L., and N. F. Marshall, Submarine canyons: internal wave traps?, *Geophys. Res. Lett.*, *3***,** 622-624, 1976.

Hickey, B. M., Patterns and processes of circulation over the Washington continental shelf and slope, in *Coastal Oceanography of Washington and Oregon*, Vol. 47, edited by M. R. Landry and B. M. Hickey, pp. 41-115, Elsevier**,** Amsterdam, 1989.

Hickey, B. M., Coastal submarine canyons, in *Proc. 'Aha Huliko'a , Hawaiian Winter Workshop, Topographic Effects in the Ocean*, pp. 95-110, School of Ocean and Earth Science and Technology, Univ. of Hawaii at Manoa, Honolulu, HI, 1995.

Hickey, B. M., The response of a steep-sided, narrow canyon to time-variable wind forcing, *J. Phys. Oceanogr.*, *27***,** 697-726, 1997.

Holloway, P. E., A Numerical Model of Internal Tides with Application to the Australian North West Shelf, *J. Phys. Oceanogr.*, *26***,** 21-37, 1996.

Hotchkiss, F. S., and C. H. Wunsch, Internal waves in Hudson Canyon with possible geological implications, *Deep-Sea Res.*, *29***,** 415-442, 1982.

Hunkins, K., Mean and tidal currents in Baltimore Canyon, *J. Geophys. Res.*, *93***,** 6917-6929, 1988.

Munk, W., Internal waves and small scale processes, in *Evolution of Physical Oceanography*, edited by B. A. Warren and C. Wunsch, pp. 264-291, MIT Press**,** Cambridge, MA, 1981.

Noble, M., and B. Butman, The structure of subtidal currents within and around Lydonia Canyon: Evidence for enhanced cross-shelf fluctuations over the mouth of the canyon, *J. Geophys. Res.*, *94***,** 8091-8110, 1989.

Paduan, J. D., and M. S. Cook, Mapping surface currents in Monterey Bay with CODAR-type HF radar, *Oceanography*, *10***,** 49-52, 1997.

Petruncio, E.T., Characterization of tidal currents in Monterey Bay from remote and in-situ measurements, *M.S. Thesis*, Dept. of Oceanography, Naval Postgraduate School, Monterey, CA, 113 pp., 1993.

Petruncio, E. T., Observations and modeling of the internal tide in a submarine canyon, *Ph.D. dissertation*, Dept. of Oceanography, Naval Postgraduate School,Monterey, CA, 181 pp., 1996.

Petruncio, E. T., L. K. Rosenfeld, and J. D. Paduan, Observations of the internal tide in Monterey Canyon, *J. Phys. Oceanogr.*, *28***,** 1873-1903, 1998.

Shea, R. E., and W. W. Broenkow, The role of internal tides in the nutrient enrichment of Monterey Bay, California, *Estuarine, Coastal, and Shelf Sci.*, *15***,** 57-66, 1982.

Slinn, D. N., and J. J. Riley, Turbulent mixing in the oceanic boundary layer caused by internal wave reflection from sloping terrain, *Dyn. Atmos. Oceans*, *24***,** 51-62, 1996.

Wunsch, C., and S. Webb, The climatology of deep ocean internal waves, *J. Phys. Oceanogr.*, *9***,** 235-243, 1979.